PNAS PLUS

# Mechanical stimulation induces formin-dependent assembly of a perinuclear actin rim

Xiaowei Shao[a,1], Qingsen Li[a,1], Alex Mogilner[b], Alexander D. Bershadsky[a,c,2], and G. V. Shivashankar[a,d,e,2]

[a]Mechanobiology Institute, National University of Singapore, 117411 Singapore; [b]Courant Institute and Department of Biology, New York University, New York, NY 10012; [c]Department of Molecular Cell Biology, Weizmann Institute of Science, Rehovot 76100, Israel; [d]Department of Biological Sciences, National University of Singapore, 117543 Singapore; and [e]FIRC Institute of Molecular Oncology, Milan 20139, Italy

Edited by Thomas D. Pollard, Yale University, New Haven, CT, and approved April 6, 2015 (received for review March 11, 2015)

**Cells constantly sense and respond to mechanical signals by reorganizing their actin cytoskeleton. Although a number of studies have explored the effects of mechanical stimuli on actin dynamics, the immediate response of actin after force application has not been studied. We designed a method to monitor the spatiotemporal reorganization of actin after cell stimulation by local force application. We found that force could induce transient actin accumulation in the perinuclear region within ∼2 min. This actin reorganization was triggered by an intracellular $Ca^{2+}$ burst induced by force application. Treatment with the calcium ionophore A23187 recapitulated the force-induced perinuclear actin remodeling. Blocking of actin polymerization abolished this process. Overexpression of Klarsicht, ANC-1, Syne Homology (KASH) domain to displace nesprins from the nuclear envelope did not abolish $Ca^{2+}$-dependent perinuclear actin assembly. However, the endoplasmic reticulum- and nuclear membrane-associated inverted formin-2 (INF2), a potent actin polymerization activator (mutations of which are associated with several genetic diseases), was found to be important for perinuclear actin assembly. The perinuclear actin rim structure colocalized with INF2 on stimulation, and INF2 depletion resulted in attenuation of the rim formation. Our study suggests that cells can respond rapidly to external force by remodeling perinuclear actin in a unique $Ca^{2+}$- and INF2-dependent manner.**

force | mechanotransduction | calcium | formin | perinuclear actin rim

Cells can sense and adapt to their physical microenvironment through specific mechanosensing mechanisms. These properties are often mediated by the actin cytoskeleton, which can be modulated by a wide range of forces. Fluid shear stress, for example, induces actin stress fiber assembly and realignment along the direction of flow (1–4), whereas the cyclic stretch of an elastic substrate induces a reorientation of stress fibers under some angle to the direction of stretch (5–8). Applying mechanical force to cells by a microneedle results in focal adhesion growth and activation of formin-type actin nucleators (9, 10). Similarly, local application of force through fibronectin or collagen-coated beads trapped by optical or magnetic tweezers leads to the local reorganization of the actin cytoskeleton. This response is associated with reinforcement of bead attachment (11), recruitment of additional actin-associated proteins (12), and activation of a variety of signaling pathways (13–17). Most studies to date have explored the effects of force on actin structures directly associated with the sites of force application, such as focal adhesions and stress fibers. However, the immediate effect of force on the assembly of actin structures distal from the sites of force application has not been assessed. Such process is despite distal effects having potential implications in the transduction of local forces from the cell periphery to nuclear events (18).

In this study, we used a local mechanical force application device and examined the large-scale actin reorganization during and after force application. Remarkably, we identified reversible actin polymerization in the perinuclear region within 1 min after mechanical stimulation. Intracellular $Ca^{2+}$ bursts were found to be essential for the perinuclear actin response. Furthermore, we showed that a potent actin polymerization factor, inverted formin-2 (INF2), was involved in the perinuclear actin remodeling. Specifically, INF2 colocalized with a transient actin structure in the perinuclear region. A reduction in the level of INF2 resulted in the attenuation of this actin remodeling process. This work reveals a previously unidentified mechanotransduction response, whereby external mechanical stimulation induces a rapid transient perinuclear actin polymerization mediated by $Ca^{2+}$ and formin.

## Results

**Force Application at the Cell Periphery Induces Reversible Perinuclear Actin Polymerization.** To investigate how actin structures respond to external force, we applied a force to NIH 3T3 cells using a specially designed micromanipulation probe [an atomic force microscopy (AFM) tip attached to a 4.5-μm bead]. The AFM tip, mounted on an x-y-z dimensional micromanipulator stage, was brought in contact with the cell periphery at an angle of ∼45° (Fig. 1*A*). The magnitude of force was estimated to be 100–200 nN by calibration using a variant of traction force microscopy (19). On force application, EGFP-Lifeact–labeled F-actin (20) was found to transiently accumulate at the perinuclear region (Fig. S1*A*), forming a rim around the nucleus (indicated by an arrow in Fig. 1*B*). Remarkably, this assembly of F-actin occurred not only at the nuclear rim, where it seemed to be the most prominent response, but also, across the entire perinuclear cytoplasmic region, where endoplasmic reticulum (ER) is abundant (Figs. S1*A* and S2 *A* and *B*).

In all additional experiments, actin intensity was measured within perinuclear regions, such as the region marked by the rectangular

### Significance

Cells can sense and adapt to their physical microenvironment through specific mechanosensing mechanisms. These properties are often mediated by the actin cytoskeleton, which can be affected by a wide range of forces, including fluid shear stress, cyclic stretch, and optical or magnetic force. However, the immediate effects of force on the assembly of actin structures distal from the sites of force application were not assessed. Our work reveals a previously unidentified actin structure, a perinuclear actin rim, which is induced by mechanical stimulation of cells. We show that, on local force application to the cell periphery, a distal effect emerges at the perinuclear region. Such distal effects have potential implications in modulating nuclear functions by local mechanical signals from the cell periphery.

Author contributions: X.S., Q.L., A.D.B., and G.V.S. designed research; X.S. and Q.L. performed research; X.S., Q.L., and A.M. contributed new reagents/analytic tools; X.S., Q.L., A.M., A.D.B., and G.V.S. analyzed data; and X.S., Q.L., A.M., A.D.B., and G.V.S. wrote the paper.

The authors declare no conflict of interest.

This article is a PNAS Direct Submission.



[1]X.S. and Q.L. contributed equally to this work.

[2]To whom correspondence may be addressed. Email: alexander.bershadsky@weizmann.ac.il or shiva.gvs@gmail.com.

This article contains supporting information online at www.pnas.org/lookup/suppl/doi:10.1073/pnas.1504837112/-/DCSupplemental.

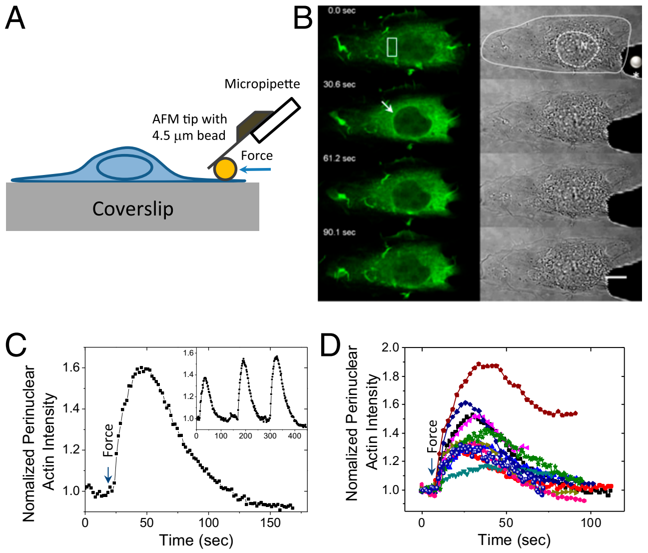


**Fig. 1.** Force-induced reversible perinuclear actin assembly. (*A*) Schematic depicting the experimental setup for the mechanical stimulation of cells. (*B*) Time-lapse images showing changes in perinuclear actin intensity on stimulation by the force probe. Cell and nucleus (N) boundaries as well as the position of the bead (*) are marked on the top bright field image. The arrow indicates the perinuclear actin rim. (Scale bar: 10 μm.) (*C*) Plots of normalized perinuclear actin intensity vs. time measured in the region shown by a white box in *B* (corresponding to a single mechanical stimulation). (*Inset*) Three subsequent stimulations of the same cell. (*D*) Plots of normalized perinuclear actin intensity from 11 independent experiments.

box in Fig. 1*B*. These measurements represented the behavior of perinuclear actin at both the nuclear rim and perinuclear ER (Fig. S2 *A* and *B*). F-actin continued to decline at the cell periphery, where ER is undetectable (Fig. S2*C*), and this phenomenon occurred concomitantly with transient perinuclear actin remodeling (Fig. S2 *D* and *E*). The time plot in Fig. 1*C* represents changes in the amount of F-actin in the perinuclear region shown in Fig. 1*B*. Here, the level of F-actin increased to its maximum after 30 s and returned to its initial level within 2 min. The intensity of perinuclear F-actin in single cells subjected to several successive stimulations is plotted in Fig. 1*C*, *Inset*. Repeated stimulation resulted in a similar accumulation of perinuclear actin (Movie S1). Actin remodeling patterns were reproducible in different cells, albeit with moderate variations of the timing and the response magnitude of the perinuclear actin accumulation (Fig. 1*D*). On average, the perinuclear F-actin signal increases 1.4 ± 0.1-fold compared with the original actin density. The rise of signal had a half-time of 6.6 ± 0.6 s, and return to its initial value occurred with the half-time of 23.4 ± 1.4 s.

By fixing the cells immediately after mechanical stimulation, the transient force-induced perinuclear actin structure could be labeled by phalloidin, indicating the presence of polymerized (F-) actin (Fig. S1*B*). Moreover, the actin bundling protein α-actinin was found to localize to the perinuclear region simultaneously with actin (Fig. S1*C*).

Formation of the perinuclear actin rim was triggered by force as well when cells were attached to a poly-L-lysine–coated substrate rather than fibronectin, indicating that the effect is not dependent on integrin-mediated adhesions (Fig. S3*A*). Accordingly, inhibition of focal adhesion kinase activity by treatment with 10 μM PF-562,271 (21) did not prevent force-induced perinuclear actin remodeling (Fig. S3*B*).

**$Ca^{2+}$ Is Essential for Force-Induced Perinuclear Actin Remodeling.** Because mechanical stimulation of fibroblast-like NIH 3T3 cells was shown to be accompanied by activation of $Ca^{2+}$ channels (22–24), we next tested the involvement of $Ca^{2+}$ signaling in force-triggered perinuclear actin remodeling. Actin and $Ca^{2+}$ were monitored simultaneously by cotransfecting cells with RFP-Lifeact and the $Ca^{2+}$ indicator G-CaMP (25). The time-lapse sequences are shown in Fig. 2*A*, and Fig. 2*B* shows a high-magnification visualization of perinuclear actin. Force application triggered an immediate increase in the level of intracellular $Ca^{2+}$ (up to 4.7 ± 1.1-fold), which propagated from the site of force application throughout the whole cell body. This $Ca^{2+}$ burst, with a half-time of 2.4 ± 0.4 s, preceded the assembly of perinuclear actin. Intracellular $Ca^{2+}$ levels subsequently returned to their basal level, and this phenomenon was accompanied by a reduction of perinuclear actin and a disappearance of the actin rim (Fig. 2 *A* and *C* and Movie S2). To examine whether $Ca^{2+}$ influx is required for perinuclear actin rim assembly, cells were incubated with 2 mM EGTA before and during force application to deplete $Ca^{2+}$ from the culture medium. Perinuclear actin remodeling was not observed in this condition (Fig. 2 *D* and *E*), suggesting that extracellular $Ca^{2+}$ is necessary for triggering this phenomenon.

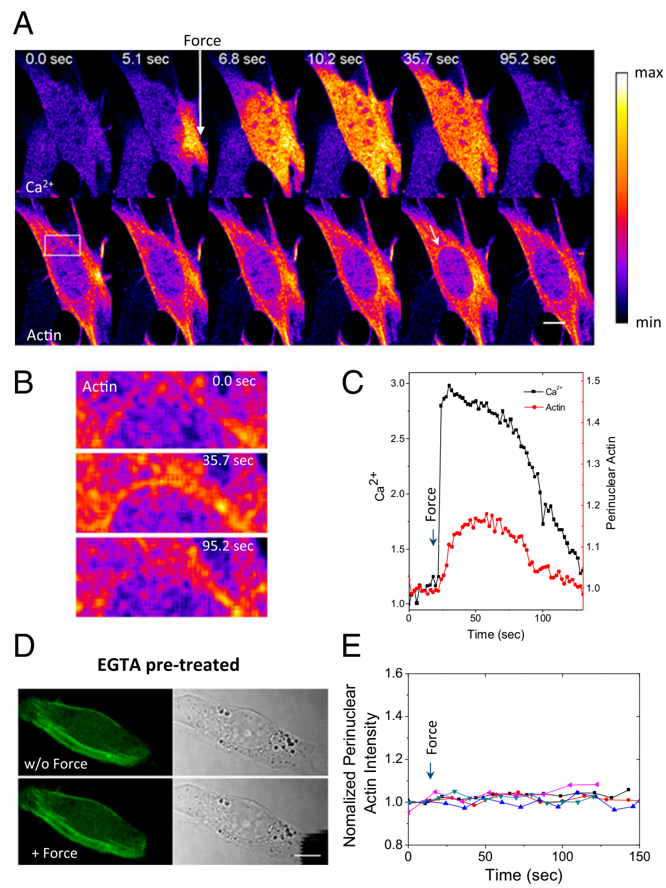


**Fig. 2.** Force-induced $Ca^{2+}$ influx precedes perinuclear actin assembly. (*A*) Time-lapse images showing fluorescence intensity of (*Upper*) the $Ca^{2+}$ indicator G-CaMP (a fusion of green fluorescent protein, calmodulin, and M13, a peptide sequence from myosin light chain kinase) and (*Lower*) red fluorescent protein (RFP)-Lifeact on force application. The color-coded images are shown in fire scale (shown on the right) and were prepared using ImageJ. The arrow in *Lower* indicates the perinuclear actin rim. (*B*) High-magnification image of the perinuclear actin rim from the region indicated by the white rectangle in *A* at different time points. (*C*) Plots of normalized perinuclear actin intensity and corresponding perinuclear $Ca^{2+}$ level as a function of time. (*D*, *Left*) Fluorescence and (*D*, *Right*) phase-contrast images of an EGFP-Lifeact–labeled cell incubated in medium containing 2 mM EGTA before and after force application. (*E*) Plots of normalized perinuclear actin intensity in five EGTA-incubated cells on force application. (Scale bars: 10 μm.)

To further examine the role of $Ca^{2+}$ in perinuclear actin remodeling, the calcium ionophore A23187 was used instead of the mechanical force to induce $Ca^{2+}$ influx. As expected, the addition of 2 μM A23187 led to an immediate increase in the overall intracellular level of $Ca^{2+}$ (up to 2.6 ± 0.3-fold) together with perinuclear actin remodeling, which is shown in Fig. 3*A* and Movie S3. The temporal dynamics of both $Ca^{2+}$ and perinuclear actin was found to be a few seconds slower than that observed after the application of force (Fig. 3*B* and Table S1). Furthermore, the release of $Ca^{2+}$ from intracellular $Ca^{2+}$ stores after an addition of the $Ca^{2+}$-ATPase inhibitor, thapsigargin (26, 27), also induced a $Ca^{2+}$ burst and perinuclear actin rim formation (Fig. 3*C*). The role of $Ca^{2+}$ in the induction of perinuclear actin assembly can also be shown in experiments where G-actin was added to digitonin-permeabilized cells (28). Here, incorporation of G-actin into the perinuclear actin rim required $Ca^{2+}$ in the buffer (Fig. S3 *C* and *D*). Thus, we conclude that $Ca^{2+}$ signaling plays a critical role in the force-stimulated assembly of perinuclear actin.

**Actin Polymerization Is Required for Perinuclear Actin Remodeling.** To understand how perinuclear actin remodeling depends on the status of actin polymerization, several methods were used to perturb actin dynamics. To allow the simultaneous visualization of multiple cells, we chose to stimulate perinuclear actin remodeling using the calcium ionophore A23187 instead of mechanical force. In the control group, 2 μM A23187 induced an increase in perinuclear actin intensity up to 1.6 ± 0.1-fold compared with untreated cells (Fig. 4*A*). The perinuclear F-actin rim was localized at the cytoplasmic side of the nuclear membrane (Fig. S4*A*). Unlike the perinuclear actin, F-actin signal inside the nucleus was very weak and did not change significantly on treatment of A23187. Of 11 cells, in which perinuclear actin showed strong increase (more than 1.5-fold of basal level), intranuclear F-actin signal increased very slightly in only 4 cells.

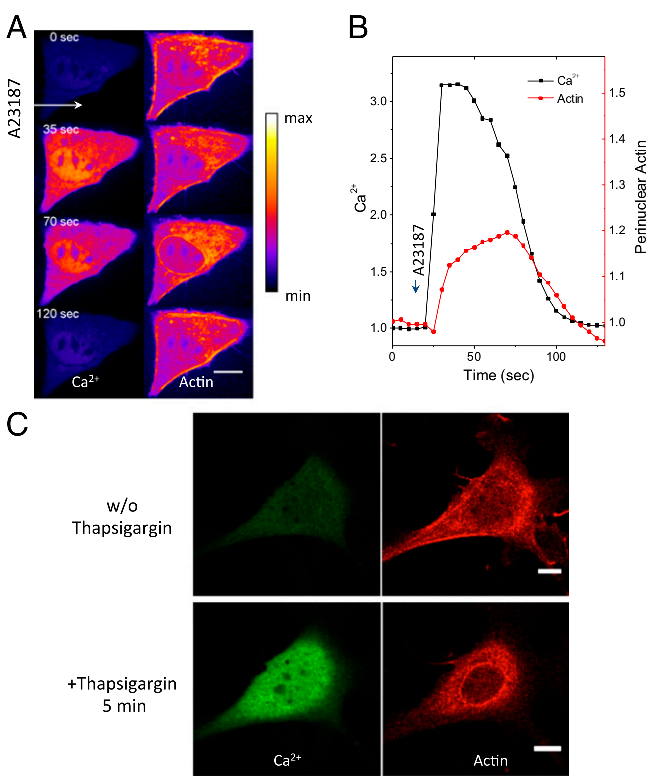


**Fig. 3.** Effect of altering $Ca^{2+}$ concentration on perinuclear actin assembly. (*A*) Time-lapse images of $Ca^{2+}$ (G-CaMP; a fusion of green fluorescent protein, calmodulin, and M13, a peptide sequence from myosin light chain kinase) and actin [red fluorescent protein (RFP)-Lifeact] on addition of the calcium ionophore A23187. A23187 was added ∼20 s after imaging commenced. The color-coded images are shown in fire scale (shown on the right) and were prepared using ImageJ. (*B*) Plots of normalized perinuclear actin intensity and the corresponding $Ca^{2+}$ level as a function of time. (*C*) Fluorescence images of $Ca^{2+}$ (G-CaMP) and actin (RFP-Lifeact) in a cell before and 5 min after the addition of 1.5 μM thapsigargin. (Scale bars: 10 μm.)

When treated with the actin-depolymerizing drug Cytochalasin D, perinuclear actin remodeling by A23187 was completely inhibited (Fig. 4*B*). Treatment with various concentrations of another actin-depolymerizing drug, Latrunculin A, alone did not alter perinuclear actin (Fig. S5 *A*–*D*) but did prevent its increase on addition of A23187 (Fig. S5*E*). A decrease in the G/F-actin ratio also inhibited perinuclear actin remodeling with treatment with A23178 (Fig. 4 *C* and *D*). In these experiments, the G/F-actin ratio was decreased when cells were treated with the actin-stabilizing drug Jasplakinolide or a potent actin polymerization factor, constitutively active formin mDia1 (ΔN3), was overexpressed. These results show that the formation of a perinuclear actin rim, whether on mechanical stimulation or calcium ionophore treatment, is the result of actin polymerization.

To determine whether factors that commonly regulate actin dynamics were also involved in force/$Ca^{2+}$-induced perinuclear actin assembly, we inhibited several regulators of actin dynamics, including the Arp2/3 complex, Rho GTPase, Rho kinase, and myosin II. To do this, CK-666, C3 transferase, Y27632, and blebbistatin, respectively, were used. However, none of these inhibitors produced any significant effect on perinuclear actin assembly (Fig. S6 *A* and *B*). Moreover, neither myosin IIA nor IIB was localized to perinuclear actin rim (Fig. S4*B*). Similarly, siRNA-mediated reduction of the expression level of cofilin-1, which is one of the major actin depolymerization factors in these cells (29), also showed no significant effect (Fig. S6 *C*–*E*). This evidence suggests that pathways leading to Arp2/3, myosin II, cofilin, or Rho activation are not involved in the process of force/$Ca^{2+}$-induced perinuclear actin assembly.

**INF2 Plays a Critical Role in Perinuclear Actin Remodeling.** To identify which molecular regulators are involved in the force/$Ca^{2+}$-induced formation of the perinuclear actin rim, we examined several actin-associated proteins that localize to the nuclear envelope and/or perinuclear area independently of stimulation. In particular, we investigated the roles of nesprins, filamin A, and the formin, INF2.



Nesprins are an essential component of the LINC complex (complex that links the nucleoskeleton and cytoskeleton), where they connect the cytoskeleton to the nuclear envelope by interactions with SUN family proteins (30). These interactions are mediated by the nesprin Klarsicht, ANC-1, Syne Homology (KASH) domain and can be uncoupled by the overexpression of a construct encoding the KASH domain (31). For this reason, we overexpressed a GFP-fused KASH domain of mouse nesprin 1*α* (31) and showed that such overexpression, indeed, removed nesprin 2 from the nuclear envelope (Fig. S7*A*). However, cells with depleted nesprin 2 still responded to A23187 treatment by forming a prominent perinuclear actin rim (Fig. S7*A*). This result suggests that nesprin 2 and probably, other nesprins are dispensable for perinuclear actin rim formation.

Filamin A was previously shown to be recruited to the perinuclear area by an interaction with refilinB (32), and indeed, we found that filamin A is enriched at the nuclear envelope region, irrespective of $Ca^{2+}$ or mechanical stimulation in NIH 3T3 cells (Fig. S7*B*). To check whether filamin A is involved in the formation of the perinuclear actin rim, we used filamin A KO mouse embryonic fibroblast cells (33). However, even in filamin A KO cells, the perinuclear actin rim assembly was still observed after stimulation with A23187 (Fig. S7*C*).

Members of the formin family of proteins are potent actin filament nucleating and elongating factors. INF2 was shown to

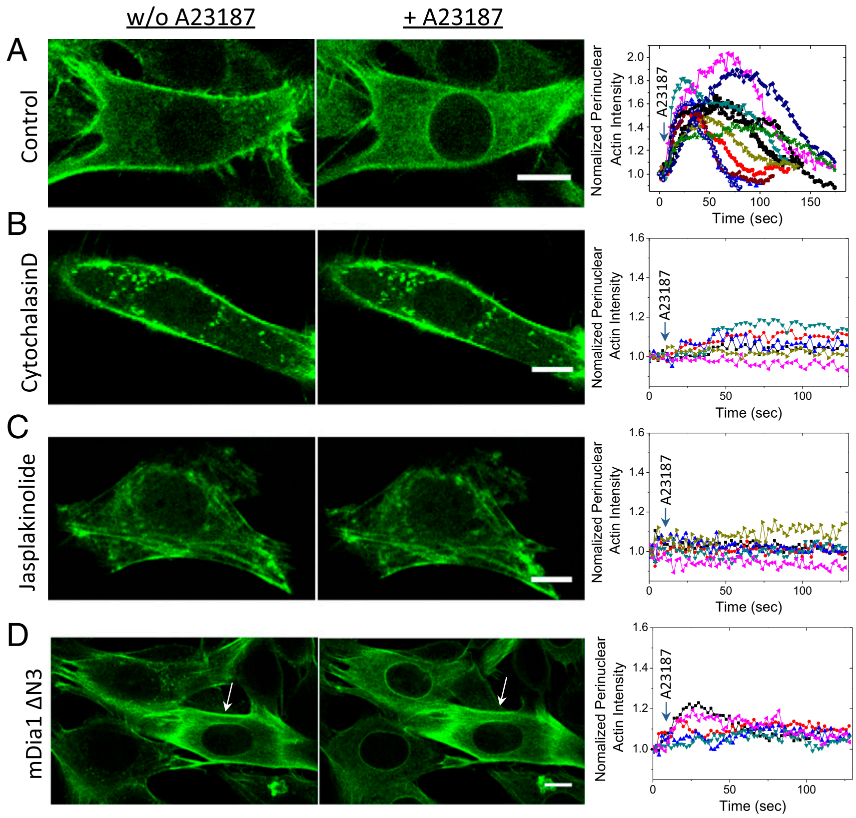


**Fig. 4.** Effect of $Ca^{2+}$ entry on perinuclear actin assembly in cells treated with different actin modulators. (*A*) Fluorescence images of EGFP-Lifeact before and after the addition of A23187 and plots of normalized perinuclear actin intensity in 11 control cells on such treatment. All curves were normalized to one at the starting points. A23187 was added ∼5 s after imaging commenced. (*B–D*) EGFP-Lifeact fluorescence images of cells pretreated with (*B*) Cytochalasin D or (*C*) Jasplakinolide or (*D*) expressing mDia1 ΔN3 (*Left*) before and (*Center*) after the addition of A23187 and (*Right*) corresponding plots of normalized perinuclear actin intensity over time in five, six, and five cells, respectively. Arrows in *D* indicate mDia1 ΔN3-transfected cell. (Scale bars: 10 μm.)

be associated with the ER (34) and constitutively localized to the perinuclear region (images in refs. 34 and 35). The antibody to INF2 revealed localization of this molecule to the perinuclear area with some enrichment at the nuclear envelope (Fig. 5*A*).

Without stimulation, there was minimal actin localization to the perinuclear area (Fig. 5*A*, *Upper*). However, after A23187 treatment, F-actin was accumulated at the perinuclear region, where it colocalized with INF2 (Fig. 5*A*, *Lower*). Based on this colocalization, we further examined the role of INF2 in the assembly of the perinuclear actin rim. INF2 was knocked down by mouse INF2 siRNA expression (SMARTpool; GE Dharmacon) to about 35% of its basal level, which was revealed by Western blotting (Fig. 5*B*). The SMARTpool siRNAs include four different siRNA sequences against mouse INF2. When expressed separately, siRNA 1, 2, 3, and 4 showed bulk, Western-blotting assessed knockdown effects of ∼35%, 50%, 82%, and 23%, respectively (Fig. 5*B*). These differences corresponded to different transfection efficiency rather than different levels of INF2 depletion in transfected cells, which was revealed by immunofluorescence INF2 staining. INF2 knockdown reduced the increase of perinuclear actin induced by A23187 treatment (Fig. 5*D*, *Upper*). Overexpression of human GFP-INF2 in INF2 siRNA 3 knocked down cells (Fig. 5*C*) rescued the perinuclear actin-positive phenotype (Fig. 5*D*, *Lower*). We further quantified the level of perinuclear actin in control, INF2 knockdown, and overexpressing/rescued cells. Without A23187, there was no significant difference in the perinuclear actin intensity in control cells, INF2 knockdown cells, and INF2-overexpressing cells (Fig. 5*E*, bars 1–3). These data suggested the expression level of INF2 did not determine perinuclear actin intensity under normal conditions. After the addition of A23187, however, INF2 knockdown cells showed a significantly lower level of perinuclear actin compared with control cells (Fig. 5*E*, bars 4–8). Rescue of knockdown cells by overexpressing GFP-INF2 significantly increased the level of perinuclear actin in A23187-treated cells (Fig. 5*E*, bar 9). Together, these results strongly indicate that INF2 plays a critical role in $Ca^{2+}$-stimulated perinuclear actin remodeling.

## Discussion

In this study, we have revealed a previously unidentified actin structure, the perinuclear actin rim, which is formed on mechanical stimulation of cells. Specifically, the local application of a force to the cell periphery initiates a transient actin polymerization at the perinuclear region. This transient actin structure was observed using the fluorescent F-actin markers Lifeact (20) and phalloidin, and its formation was prevented by treatments inhibiting actin polymerization. The cross-linking protein $\alpha$-actinin colocalizes with actin immediately during the perinuclear rim assembly, and therefore, the newly polymerized perinuclear actin likely assembles into a cross-linked network. Neither myosin IIA nor myosin IIB was found to be associated with the perinuclear actin rim, and inhibition of myosin II contractility did not affect formation of this actin structure. Although various studies have reported observations of actin reorganization on mechanical stimuli (1–11, 14–17), the transient perinuclear actin polymerization is revealed here for the first time to our knowledge.

Although many studies suggest that integrin signaling plays an important role in the cellular response to mechanical stimuli (9, 13, 17), we found that the force-induced perinuclear actin remodeling was not dependent on integrin signaling. Indeed, neither the suppression of focal adhesion formation by inappropriate substrates nor the inhibition of focal adhesion kinase affected the perinuclear actin response.

As shown previously, mechanical stimulation of cells can trigger an increase in cytosolic $Ca^{2+}$ concentration (22–24, 36, 37). Using a genetically encoded $Ca^{2+}$ indicator G-CaMP (25), we monitored cellular $Ca^{2+}$ concentration on force application and found that there was a $Ca^{2+}$ burst before the perinuclear actin assembly. Treatment with the calcium ionophore A23187 as well

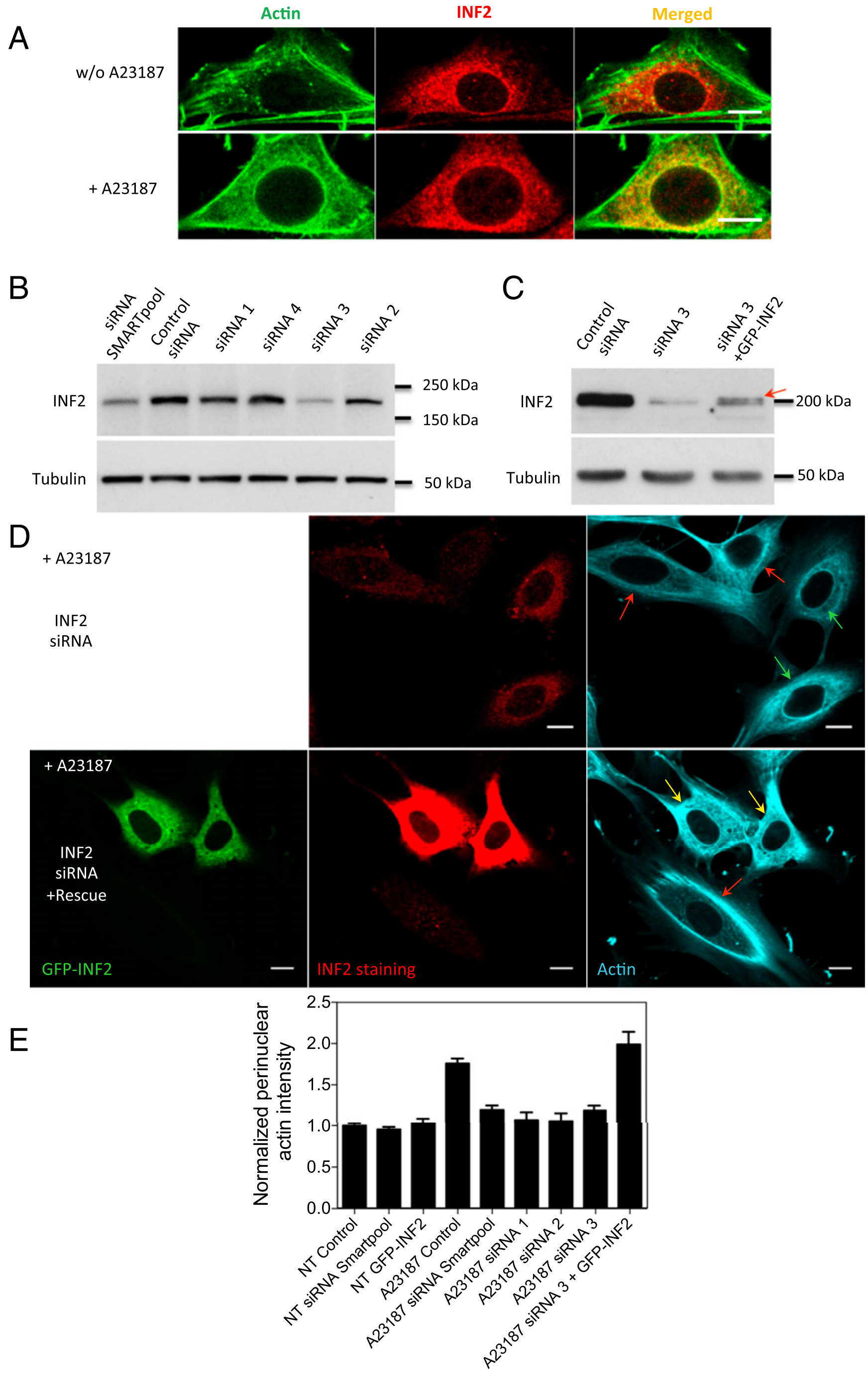


**Fig. 5.** Function of INF2 in perinuclear actin assembly. (*A*) Fluorescence staining of F-actin (phalloidin; green) and INF2 (red) in (*Upper*) nontreated and (*Lower*) A23187-treated cells. Merged images are shown in *Right*. (*B*) Immunoblots of INF2 in control and knockdowns. INF2 siRNA SMARTpool as well as siRNA 1, 2, and 3 all show a significant knockdown effect compared with control siRNA. Tubulin content is shown as an internal control. (*C*) Immunoblots of INF2 in control, siRNA 3 knockdown, and GFP-INF2–rescued cells. The exogenous fraction of INF2 is labeled by an arrow. (*D*) Fluorescence staining of F-actin (phalloidin; cyan) and INF2 (red) in control cells (green arrows), INF2 knockdown cells (red arrows), and GFP-INF2–rescued cells (yellow arrows) on A23187 treatment. (*E*) Normalized perinuclear actin intensity in nontreated (bar 1–3) or A23187-treated (bar 4–9) control, INF2 knockdown, and INF2-overexpressing/rescued cells. All data were first normalized by A23187-treated control cells from each corresponding experiment and then divided by the mean value of the nontreated (NT) control group. More than 10 cells were used for the measurements in each type of treatment. Data are presented as means ± SEM. (Scale bars: 10 μm.)

as the intracellular $Ca^{2+}$-ATPase inhibitor thapsigargin faithfully reproduced the perinuclear actin remodeling induced by mechanical stimulation. Thus, the reorganization of the perinuclear actin is probably triggered by $Ca^{2+}$ entry either through stretch-sensitive channels (36, 37) or because of a reversible membrane rupture (38) during force application.

Downstream to an increased $Ca^{2+}$ concentration, two types of molecular regulators could affect actin assembly in the perinuclear region: actin polymerization factors and proteins linking actin filaments to the nucleus. We found that the Arp2/3 complex, which is a well-known actin nucleation factor, was not involved in the perinuclear actin remodeling. We also showed that the actin cross-linking protein filamin A was dispensable for this actin remodeling process, although it has been implicated in perinuclear actin organization (32). Furthermore, we showed that depletion of endogenous nesprins, the actin binding proteins connecting the nuclear envelope with the actin cytoskeleton, did not abolish this response. Finally, the important regulator of actin dynamics, cofilin, which has been shown to be activated by $Ca^{2+}$ (39), was also found to be nonessential in the perinuclear actin assembly.

However, a member of the formin family, INF2, was found to influence the formation of the perinuclear actin rim. INF2 is known to associate with ER (34), but it is also enriched at the perinuclear region and in particular, the nuclear envelope. Because colocalization of INF2 with F-actin was observed at the perinuclear region on $Ca^{2+}$ stimulation, the role of INF2 in perinuclear actin polymerization was examined. siRNA silencing of INF2 significantly attenuated the $Ca^{2+}$-induced perinuclear actin remodeling, which can be rescued by expression of exogenous INF2. Importantly, the overexpression of INF2 without $Ca^{2+}$ stimulation did not induce the perinuclear actin rim. Together, these results show that the force-induced perinuclear actin reorganization is mediated by $Ca^{2+}$ signaling and involves INF2. Possible roles of other formins in the perinuclear actin assembly still deserve to be studied.

The mechanisms that could activate formin-driven perinuclear actin polymerization after mechanical stimulation and $Ca^{2+}$ burst are not clear. In principle, $Ca^{2+}$ can either directly or indirectly activate INF2-driven perinuclear actin polymerization. Numerous data indicate that $Ca^{2+}$ can promote the disassembly of actin structures through pathways that involve cofilin and gelsolin (39, 40). We, therefore, considered the hypothesis that a burst of perinuclear actin polymerization results from an increase in the level of G-actin after $Ca^{2+}$-dependent actin filament disassembly. A cofilin-dependent but surprisingly, $Ca^{2+}$-independent increase in G-actin levels was detected in *Xenopus* XTC cells after mechanical stimulation (10). Additionally, it was shown that G-actin can activate formin mDia1 (41) and INF2 (42). Thus, in our initial model, we assumed that mechanical stimulation induces an increase in the level of G-actin, which in turn, activates INF2 located in the perinuclear area, and that this leads to actin polymerization.

To check whether this hypothesis can predict the time course observed for transient perinuclear actin growth, we translated these qualitative hypotheses into equations for actin concentrations at the perinuclear and peripheral regions. The data about dynamics of perinuclear and peripheral actin were obtained by fluorescence recovery after photobleaching (Fig. S8 *A* and *B* and Tables S2 and S3). Although the solutions (*SI Materials and Methods*) predicted a transient increase in perinuclear actin (Fig. S8*C*), the shape of the curve differs from that observed in our experiments. Moreover, an attempt to create a transient increase in the level of G-actin by adding a low concentration of Latrunculin (41) did not induce any perinuclear actin assembly. Finally, knockdown of cofilin-1, the major isoform of cofilin in the 3T3 cells and a most probable mediator of F-actin disassembly, did not produce any significant effect on the perinuclear actin assembly induced by $Ca^{2+}$. Taken together, these findings suggested that other mechanisms are responsible for INF2 activation.

It remains possible that $Ca^{2+}$ activates INF2-driven actin perinuclear polymerization independently of the increase in G-actin concentration. For example, the activity of INF2 or its immediate stimulators, such as cdc42 (43), could be regulated by $Ca^{2+}$ concentration. Such a possibility is represented by a second mathematical model, which is presented in Fig. S8*D*. This simple model shows that the assumption leads to a realistic prediction for the transient increase of perinuclear F-actin density. Furthermore, this idea is indirectly supported by our observation that incorporation of actin monomers into the perinuclear rim of permeabilized cells was $Ca^{2+}$-dependent. To explain the prolonged decrease in peripheral actin, after perinuclear actin returns to a steady state (Fig. S2*E*), additional assumptions are required. The mechanisms of INF2 activation await additional investigation.

It has been shown that the cell can respond to the mechanical characteristics of its microenvironment by stabilizing lamin A/C and regulating changes in lamin protein composition and nuclear morphology (44). The timescale of this process is significantly slower than that of the perinuclear actin polymerization described in this study (tens of minutes vs. tens of seconds). It is possible however, that a cross-talk exists between the responses of the perinuclear actin network and nuclear lamin. A possibility that formation of a perinuclear actin rim can switch nucleoskeleton dynamics deserves to be studied.

Finally, $Ca^{2+}$ dynamics and actin remodeling have been shown to play an important role in regulating the nuclear transport of several transcription factors, including nuclear factor of activated T cells, myocardin-like protein, and Yes-associated protein (16, 45–48). This property suggests that the force/$Ca^{2+}$-mediated perinuclear actin remodeling may serve as a mechanism of mechanotransduction by enabling the delivery of mechanical signals from the cytoplasm to the nucleus. On the other hand, the transient assembly of an actin-based structure around the nucleus may function as a kinetic barrier to protect genome integrity until cellular homeostasis is reestablished. Interestingly, mutations in INF2 were shown to be linked to two human diseases: focal and segmental glomerulosclerosis, a degenerative kidney disease (49), and Charcot–Marie–Tooth disease, a peripheral nervous system disorder (50). In both cases, mutations in INF2 led to a reduction of perinuclear accumulation of this formin (50). A possible role for the $Ca^{2+}$- and formin-dependent perinuclear actin rim assembly in regulating nuclear function provides an interesting avenue for future studies.

## Materials and Methods

**Cell Culture and Drug Treatment.** NIH 3T3 fibroblasts were cultured in low-glucose DMEM (Life Technologies) supplemented with 10% (vol/vol) FBS (Gibco; Life Technologies) and 1 mM penicillin-streptomycin (Life Technologies) at 37 °C with 5% $CO_2$. Immortalized mouse embryonic fibroblast cells (MEFs) (51) and FlnA ($^{-/-}$) MEFs (33) were maintained in high-glucose DMEM at the same condition. For calcium experiments, 2 mM EGTA, 2 μM calcium ionophore A23187, or 1.5 μM thapsigargin was used. For actin perturbation, 500 nM Cytochalasin D, 400 nM Jasplakinolide, or 200 nM Latrunculin A was applied for 30–40 min; 20–200 nM Latrunculin A was applied to examine the initial effect of actin depolymerization, and 25 μM blebbistatin, 100 μM CK-666, 1 μg/mL C3 transferase (Cytoskeleton), 10 μM Y-27632, and 10 μM PF-562271 (Selleck Chemicals) were used to inhibit myosin II, Arp2/3, Rho GTPase, Rho kinase, and focal adhesion kinase, respectively. All chemicals were purchased from Sigma-Aldrich, except for those specified.

**Cell Transfection.** Transfection of plasmids in WT NIH 3T3 cells was carried out using the Lipofectamine Plus Kit (Life Technologies) or Fugene HD (Roche). EGFP-Lifeact (20) and RFP-Lifeact were gifts from Roland Wedlich-Soldner (Institute of Cell Dynamics and Imaging, University of Münster, Münster, Germany). EGFP-$\beta$-actin and EGFP-$\alpha$-actinin were used in previous work of our laboratory (52). mCherry-mDia1-ΔN3 was used and described in earlier work of our laboratory (53). G-CaMP (25), used for $Ca^{2+}$ labeling, was a gift from Min Wu (Mechanobiology Institute, National University of Singapore, Singapore). GFP-KASH (31) was a gift from Brian Burke (Institute of Medical Biology, Singapore). GFP-INF2 (isoform 1, C-terminal prenylated) was a gift from Miguel A. Alonso (Centro de Biologia Molecular Severo Ochoa, Madrid), and it was described previously (43). pDsRed2-ER vector, purchased from Clontech, was used to label ER. All transfected cells were incubated for 24–48 h before experiments.

For siRNA transfection, 10 pmol mouse INF2 siRNAs (SMARTpool and Set of 4), mouse cofilin-1 siRNAs (SMARTpool), or nontargeting control siRNAs (SMARTpool) were transfected using Lipofectamine RNAiMAX (Life Technologies) and incubated for 72–96 h before experiments. All siRNAs were purchased from GE Dharmacon.

**Mechanical Stimulation.** An atomic force microscopy (AFM) tip with a 4.5-μm polystyrene bead was attached to a glass pipette, which was controlled by an Eppendorf micromanipulator. The force probe was brought to the boundary of spreading cells, and a pushing force was applied. Live-cell imaging was captured using Zeiss 710 Confocal Microscopy during force application. Calibration of force was done in the same setup using a 3-kPa Acrylamide gel embedded with fluorescent beads (19). The force applied by the AFM tip, calculated by the displacement of the fluorescent beads and elastic modulus of the gel, was estimated to be 100–200 nN.

Details regarding immunofluorescence, immunoblotting, confocal imaging, data analysis, and mathematical modeling are also provided in *SI Materials and Methods*.

**ACKNOWLEDGMENTS.** We thank Dr. Miguel A. Alonso, Dr. Min Wu, Dr. Brian Burke, and Dr. Roland Wedlich-Soldner for gifts of plasmids and antibodies. We also thank Steven Wolf (Mechanobiology Institute, Singapore) for expert help in preparing this article for publication. All microscopy was carried out at the Microscopy Core Facility, MBI, National University of Singapore. This research was supported by the National Research Foundation, Singapore; the Ministry of Education, Singapore; and funding to the MBI, National University of Singapore. A.M. was supported by National Science Foundation Grant DMS-1118206 and NIH Grant GM068952. A.D.B. holds the Joseph Moss Professorial Chair in Biomedical Research at the Weizmann Institute and is a visiting professor at the National University of Singapore; A.D.B. acknowledges support from Israel Science Foundation Grant 956/10 and a Lord David Alliance Manchester-Weizmann Grant.

1. Franke RP, et al. (1984) Induction of human vascular endothelial stress fibres by fluid shear stress. *Nature* 307(5952):648–649.
2. Chen NX, et al. (2000) Ca(2+) regulates fluid shear-induced cytoskeletal reorganization and gene expression in osteoblasts. *Am J Physiol Cell Physiol* 278(5):C989–C997.
3. Tzima E, et al. (2005) A mechanosensory complex that mediates the endothelial cell response to fluid shear stress. *Nature* 437(7057):426–431.
4. Zaidel-Bar R, Kam Z, Geiger B (2005) Polarized downregulation of the paxillin-p130CAS-Rac1 pathway induced by shear flow. *J Cell Sci* 118(Pt 17):3997–4007.
5. Livne A, Bouchbinder E, Geiger B (2014) Cell reorientation under cyclic stretching. *Nat Commun* 5:3938.
6. Yoshigi M, Hoffman LM, Jensen CC, Yost HJ, Beckerle MC (2005) Mechanical force mobilizes zyxin from focal adhesions to actin filaments and regulates cytoskeletal reinforcement. *J Cell Biol* 171(2):209–215.
7. Kaunas R, Nguyen P, Usami S, Chien S (2005) Cooperative effects of Rho and mechanical stretch on stress fiber organization. *Proc Natl Acad Sci USA* 102(44):15895–15900.
8. Greiner AM, Chen H, Spatz JP, Kemkemer R (2013) Cyclic tensile strain controls cell shape and directs actin stress fiber formation and focal adhesion alignment in spreading cells. *PLoS ONE* 8(10):e77328.
9. Riveline D, et al. (2001) Focal contacts as mechanosensors: Externally applied local mechanical force induces growth of focal contacts by an mDia1-dependent and ROCK-independent mechanism. *J Cell Biol* 153(6):1175–1186.
10. Higashida C, et al. (2013) F- and G-actin homeostasis regulates mechanosensitive actin nucleation by formins. *Nat Cell Biol* 15(4):395–405.
11. Choquet D, Felsenfeld DP, Sheetz MP (1997) Extracellular matrix rigidity causes strengthening of integrin-cytoskeleton linkages. *Cell* 88(1):39–48.
12. Galbraith CG, Yamada KM, Sheetz MP (2002) The relationship between force and focal complex development. *J Cell Biol* 159(4):695–705.
13. Wang Y, et al. (2005) Visualizing the mechanical activation of Src. *Nature* 434(7036): 1040–1045.
14. Glogauer M, et al. (1997) Calcium ions and tyrosine phosphorylation interact coordinately with actin to regulate cytoprotective responses to stretching. *J Cell Sci* 110(Pt 1):11–21.
15. Collins C, et al. (2012) Localized tensional forces on PECAM-1 elicit a global mechanotransduction response via the integrin-RhoA pathway. *Curr Biol* 22(22):2087–2094.
16. Iyer KV, Pulford S, Mogilner A, Shivashankar GV (2012) Mechanical activation of cells induces chromatin remodeling preceding MKL nuclear transport. *Biophys J* 103(7): 1416–1428.
17. Chan MW, Chaudary F, Lee W, Copeland JW, McCulloch CA (2010) Force-induced myofibroblast differentiation through collagen receptors is dependent on mammalian diaphanous (mDia). *J Biol Chem* 285(12):9273–9281.
18. Shivashankar GV (2011) Mechanosignaling to the cell nucleus and gene regulation. *Annu Rev Biophys* 40:361–378.
19. Yip AK, et al. (2013) Cellular response to substrate rigidity is governed by either stress or strain. *Biophys J* 104(1):19–29.
20. Riedl J, et al. (2008) Lifeact: A versatile marker to visualize F-actin. *Nat Methods* 5(7): 605–607.
21. Roberts WG, et al. (2008) Antitumor activity and pharmacology of a selective focal adhesion kinase inhibitor, PF-562,271. *Cancer Res* 68(6):1935–1944.
22. Ruder WC, et al. (2012) Calcium signaling is gated by a mechanical threshold in three-dimensional environments. *Sci Rep* 2(2012):554.
23. Glogauer M, Ferrier J, McCulloch CA (1995) Magnetic fields applied to collagen-coated ferric oxide beads induce stretch-activated Ca2+ flux in fibroblasts. *Am J Physiol* 269(5 Pt 1):C1093–C1104.
24. Munevar S, Wang YL, Dembo M (2004) Regulation of mechanical interactions between fibroblasts and the substratum by stretch-activated Ca2+ entry. *J Cell Sci* 117(Pt 1):85–92.
25. Nakai J, Ohkura M, Imoto K (2001) A high signal-to-noise Ca(2+) probe composed of a single green fluorescent protein. *Nat Biotechnol* 19(2):137–141.
26. Thastrup O, Cullen PJ, Drøbak BK, Hanley MR, Dawson AP (1990) Thapsigargin, a tumor promoter, discharges intracellular Ca2+ stores by specific inhibition of the endoplasmic reticulum Ca2(+)-ATPase. *Proc Natl Acad Sci USA* 87(7):2466–2470.
27. Chao TS, Byron KL, Lee KM, Villereal M, Rosner MR (1992) Activation of MAP kinases by calcium-dependent and calcium-independent pathways. Stimulation by thapsigargin and epidermal growth factor. *J Biol Chem* 267(28):19876–19883.
28. Hirata H, Tatsumi H, Sokabe M (2008) Mechanical forces facilitate actin polymerization at focal adhesions in a zyxin-dependent manner. *J Cell Sci* 121(Pt 17):2795–2804.
29. Hotulainen P, Paunola E, Vartiainen MK, Lappalainen P (2005) Actin-depolymerizing factor and cofilin-1 play overlapping roles in promoting rapid F-actin depolymerization in mammalian nonmuscle cells. *Mol Biol Cell* 16(2):649–664.
30. Crisp M, et al. (2006) Coupling of the nucleus and cytoplasm: Role of the LINC complex. *J Cell Biol* 172(1):41–53.
31. Lombardi ML, et al. (2011) The interaction between nesprins and sun proteins at the nuclear envelope is critical for force transmission between the nucleus and cytoskeleton. *J Biol Chem* 286(30):26743–26753.
32. Gay O, et al. (2011) RefilinB (FAM101B) targets filamin A to organize perinuclear actin networks and regulates nuclear shape. *Proc Natl Acad Sci USA* 108(28):11464–11469.
33. Lynch CD, et al. (2011) Filamin depletion blocks endoplasmic spreading and destabilizes force-bearing adhesions. *Mol Biol Cell* 22(8):1263–1273.
34. Chhabra ES, Ramabhadran V, Gerber SA, Higgs HN (2009) INF2 is an endoplasmic reticulum-associated formin protein. *J Cell Sci* 122(Pt 9):1430–1440.
35. Ramabhadran V, Hatch AL, Higgs HN (2013) Actin monomers activate inverted formin 2 by competing with its autoinhibitory interaction. *J Biol Chem* 288(37):26847–26855.
36. Woo SH, et al. (2014) Piezo2 is required for Merkel-cell mechanotransduction. *Nature* 509(7502):622–626.
37. Coste B, et al. (2012) Piezo proteins are pore-forming subunits of mechanically activated channels. *Nature* 483(7388):176–181.
38. Idone V, Tam C, Andrews NW (2008) Two-way traffic on the road to plasma membrane repair. *Trends Cell Biol* 18(11):552–559.
39. Wang Y, Shibasaki F, Mizuno K (2005) Calcium signal-induced cofilin dephosphorylation is mediated by Slingshot via calcineurin. *J Biol Chem* 280(13):12683–12689.
40. Robinson RC, et al. (1999) Domain movement in gelsolin: A calcium-activated switch. *Science* 286(5446):1939–1942.
41. Higashida C, et al. (2008) G-actin regulates rapid induction of actin nucleation by mDia1 to restore cellular actin polymers. *J Cell Sci* 121(Pt 20):3403–3412.
42. Gurel PS, et al. (2014) INF2-mediated severing through actin filament encirclement and disruption. *Curr Biol* 24(2):156–164.
43. Madrid R, et al. (2010) The formin INF2 regulates basolateral-to-apical transcytosis and lumen formation in association with Cdc42 and MAL2. *Dev Cell* 18(5):814–827.
44. Buxboim A, et al. (2014) Matrix elasticity regulates lamin-A,C phosphorylation and turnover with feedback to actomyosin. *Curr Biol* 24(16):1909–1917.
45. Rivas FV, O'Keefe JP, Alegre ML, Gajewski TF (2004) Actin cytoskeleton regulates calcium dynamics and NFAT nuclear duration. *Mol Cell Biol* 24(4):1628–1639.
46. Hogan PG, Chen L, Nardone J, Rao A (2003) Transcriptional regulation by calcium, calcineurin, and NFAT. *Genes Dev* 17(18):2205–2232.
47. Dupont S, et al. (2011) Role of YAP/TAZ in mechanotransduction. *Nature* 474(7350): 179–183.
48. Aragona M, et al. (2013) A mechanical checkpoint controls multicellular growth through YAP/TAZ regulation by actin-processing factors. *Cell* 154(5):1047–1059.
49. Brown EJ, et al. (2010) Mutations in the formin gene INF2 cause focal segmental glomerulosclerosis. *Nat Genet* 42(1):72–76.
50. Boyer O, et al. (2011) INF2 mutations in Charcot-Marie-Tooth disease with glomerulopathy. *N Engl J Med* 365(25):2377–2388.
51. Giannone G, et al. (2007) Lamellipodial actin mechanically links myosin activity with adhesion-site formation. *Cell* 128(3):561–575.
52. Luo W, et al. (2013) Analysis of the local organization and dynamics of cellular actin networks. *J Cell Biol* 202(7):1057–1073.
53. Zilberman Y, et al. (2011) Involvement of the Rho-mDia1 pathway in the regulation of Golgi complex architecture and dynamics. *Mol Biol Cell* 22(16):2900–2911.